Pharmacological Stimulation of NADH Oxidation Ameliorates Obesity and Related Phenotypes in Mice

Jung Hwan Hwang,[1] Dong Wook Kim,[1] Eun Jin Jo,[2] Yong Kyung Kim,[1] Young Suk Jo,[1] Ji Hoon Park,[3] Sang Ku Yoo,[2] Myung Kyu Park,[2] Tae Hwan Kwak,[2] Young Lim Kho,[4] Jin Han,[5] Hueng-Sik Choi,[6] Sang-Hee Lee,[7] Jin Man Kim,[7] InKyu Lee,[8] Taeyoon Kyung,[9] Cholsoon Jang,[9] Jongkyeong Chung,[9] Gi Ryang Kweon,[3] and Minho Shong[1]

OBJECTIVE—Nicotinamide adenine dinucleotides (NAD^+ and NADH) play a crucial role in cellular energy metabolism, and a dysregulated NAD^+-to-NADH ratio is implicated in metabolic syndrome. However, it is still unknown whether a modulating intracellular NAD^+-to-NADH ratio is beneficial in treating metabolic syndrome. We tried to determine whether pharmacological stimulation of NADH oxidation provides therapeutic effects in rodent models of metabolic syndrome.

RESEARCH DESIGN AND METHODS—We used β-lapachone (βL), a natural substrate of NADH:quinone oxidoreductase 1 (NQO1), to stimulate NADH oxidation. The βL-induced pharmacological effect on cellular energy metabolism was evaluated in cells derived from NQO1-deficient mice. In vivo therapeutic effects of βL on metabolic syndrome were examined in diet-induced obesity (DIO) and *ob/ob* mice.

RESULTS—NQO1-dependent NADH oxidation by βL strongly provoked mitochondrial fatty acid oxidation in vitro and in vivo. These effects were accompanied by activation of AMP-activated protein kinase and carnitine palmitoyltransferase and suppression of acetyl-coenzyme A (CoA) carboxylase activity. Consistently, systemic βL administration in rodent models of metabolic syndrome dramatically ameliorated their key symptoms such as increased adiposity, glucose intolerance, dyslipidemia, and fatty liver. The treated mice also showed higher expressions of the genes related to mitochondrial energy metabolism (PPARγ coactivator-1α, nuclear respiratory factor-1) and caloric restriction (Sirt1) consistent with the increased mitochondrial biogenesis and energy expenditure.

CONCLUSIONS—Pharmacological activation of NADH oxidation by NQO1 resolves obesity and related phenotypes in mice, opening the possibility that it may provide the basis for a new therapy for the treatment of metabolic syndrome. ***Diabetes*** **58: 965–974, 2009**

From the [1]Department of Internal Medicine, Chungnam National University School of Medicine, Daejeon, Korea; the [2]Mazence Inc R&D Center, Suwon, Korea; the [3]Department of Biochemistry, Chungnam National University School of Medicine, Daejeon, Korea; the [4]Department of Environmental Health, Seoul Health College, Sungnam, Korea; the [5]Department of Physiology and Biophysics, Inje University College of Medicine, Busan, Korea; the [6]Hormone Research Center, Chonnam National University, Kwangju, Korea; the [7]Department of Pathology, Chungnam National University School of Medicine, Daejeon, Korea; the [8]Section of Endocrinology, Department of Internal Medicine, Kyungpook National University School of Medicine, Junggu, Daegu, Korea; and the [9]Department of Biological Sciences, Korea Advanced Institute of Science and Technology, Daejeon, Korea.

Corresponding authors: Minho Shong, minhos@cnu.ac.kr, and Gi Ryang Kweon, mitochondria@cnu.ac.kr.

Received 28 August 2008 and accepted 1 January 2009.

Published ahead of print at http://diabetes.diabetesjournals.org on 9 January 2009. DOI: 10.2337/db08-1183.

J.H.H. and D.W.K. contributed equally to this work.

Metabolic syndrome comprises a constellation of specific cardiovascular disease risk factors whose underlying pathophysiology is related to insulin resistance (1). All the components of metabolic syndrome such as dyslipidemia, high blood pressure, glucose intolerance, and liver and muscle fat infiltration are related to central obesity. It has been reported that the imbalance between energy intake and expenditure is clearly related to obesity and metabolic disorders (2). Less calorie intake and more energy expenditure through exercise are the most effective modalities for the prevention of metabolic syndrome (3). Calorie restriction (4) and increased physical activity, in fact, have been known to prevent and reverse the phenotypes of metabolic syndrome by activating metabolic regulator proteins such as Sirt1, AMP-activated protein kinase (AMPK), and PPARγ coactivator-1α (PGC-1α) (5–8). The protective effects of these proteins against metabolic syndrome are closely linked to increased mitochondrial functions (9,10).

Previous studies have indicated that nicotinamide adenine dinucleotides (NAD^+ and NADH) are fundamental mediators of energy metabolism (11,12). An increased intracellular level of NAD^+ activates Sirt1-dependent metabolic control, mediating the effects of calorie restriction in mammals (5). Moreover, pharmacological activation of Sirt1 prevents development of metabolic syndrome through the synergistic activation of AMPK and PGC-1α, which results in elevated mitochondrial respiration (10). Mitochondrial NADH is a critical electron donor in mitochondrial electron transport chain, and cytosolic NADH can be shuttled into mitochondria, thereby affecting mitochondrial oxidative phosphorylation. Based on these ideas, we hypothesized that transiently increased NAD^+ levels coupled with decreased NADH levels in cytosol provoke mitochondrial oxidative phosphorylation and that long-term induction of a higher NAD^+-to-NADH ratio mimics the effects of calorie restriction.

NADH:quinone oxidoreductase 1 (NQO1) is a cytosolic antioxidant flavoprotein that catalyzes the reduction of highly reactive quinone metabolites by using NADH as an electron donor (Fig. 1*A*) (13). A naturally occurring compound, β-lapachone (βL) is a substrate of NQO1 and its treatment to cancer cells results in depletion of NADH and consequent apoptosis (14). ArQule (ARQ) 501, a synthetic version of βL, is a promising anticancer drug currently in multiple phase II clinical trials. Its anticancer action is

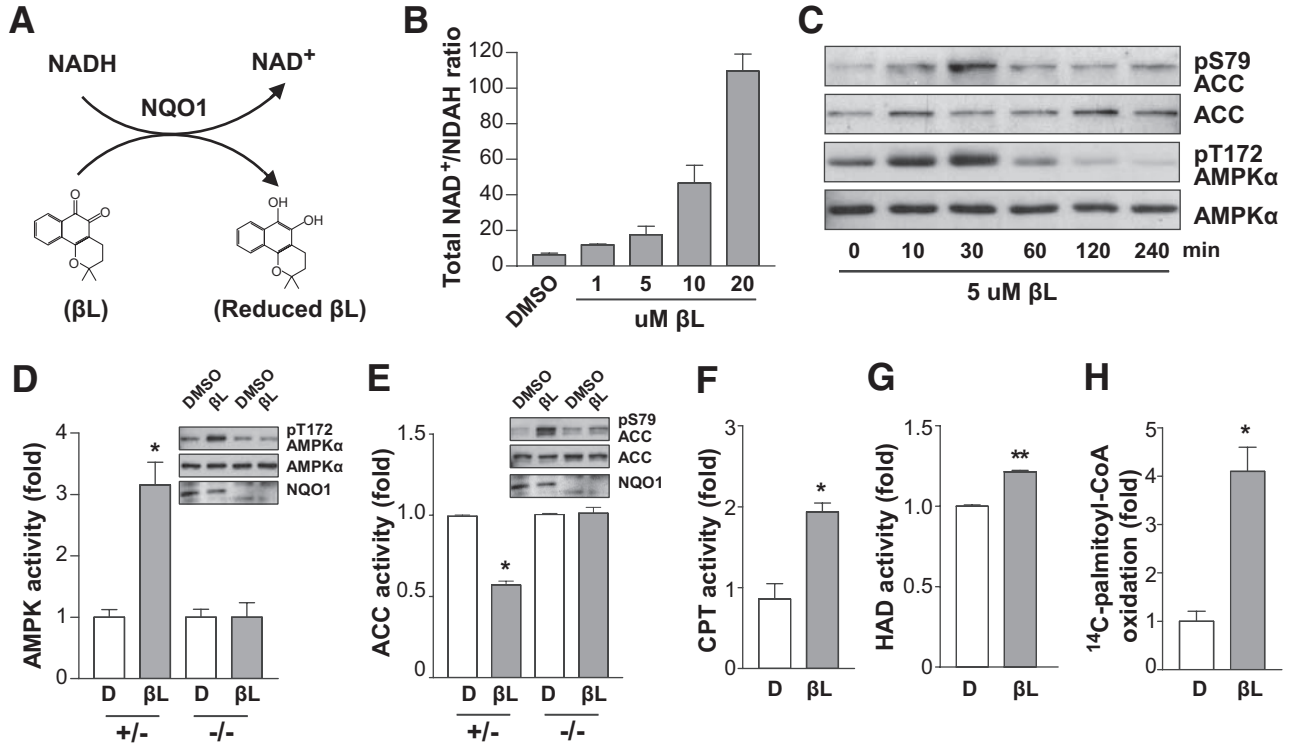

FIG. 1. βL-induced NADH oxidation stimulates the AMPK signaling pathway and mitochondrial fuel metabolism in NQO1-expressing cells. *A*: Schematic illustration of NQO1-mediated chemical reaction. NADH is oxidized by providing two electrons to βL, which is catalyzed by NQO1. *B*: L6 myoblasts were treated with the indicated concentration of βL for 30 min and extracted in lysis buffer containing 80% ice-cold methanol/water ($MtOH/H_2O$). Representative NAD^+-to-NADH ratios were determined by liquid chromatography–mass spectroscopy/mass spectroscopy analysis as described in RESEARCH DESIGN AND METHODS. All experiments were performed in triplicate. *C*: βL-induced phosphorylations of AMPKα and ACC. Immunoblot analyses of the lysates from MEF treated with βL (5 μmol/l) for the indicated time periods were performed with antibodies to the indicated proteins. *D*: Phosphorylation and activation of AMPK by βL in $NQO^{+/-}$ and $NQO1^{-/-}$ MEFs. Phosphorylation of AMPKα was estimated by immunoblot analyses of the lysates from $NQO^{+/-}$ and $NQO1^{-/-}$ MEF treated with βL (5 μmol/l) or DMSO for 30 min, and the activity of AMPK was measured by using the SAMS peptide assay. Error bars indicate SD. *E*: Phosphorylation of ACC was estimated by immunoblot analyses of the lysates from $NQO^{+/-}$ and $NQO1^{-/-}$ MEF treated with βL (5 μmol/l) or DMSO for 30 min, and the activity of ACC was determined by quantifying the fixation of $^{14}CO_2$ to acid-stable products. *F–H*: Comparison of CPT (*F*), 3-HAD (*G*) activities, or ^{14}C-palmityl-CoA oxidation (*H*) between DMSO- and βL-treated L6 myoblasts. Error bars indicate SD (*$P < 0.05$; **$P < 0.005$).

based on the findings that cancer cells usually exhibit a high level of NQO1 expression. In this study, we investigate the effect of βL on the metabolic syndrome of rodent models to examine whether pharmacological induction of a high NAD^+-to-NADH ratio is beneficial in treating the key components of metabolic syndrome.

RESEARCH DESIGN AND METHODS

Animal models. All animal procedures were in accordance with the guidelines issued by the Institutional Animal Care and Use Committee of the Chungnam National University School of Medicine. Otsuka Long Evans Tokushima fatty rats were from the Otsuka Research Institute. Male *ob/ob* and C57BL/6 mice were from The Jackson Laboratory and housed four per cage in a room maintained at a constant temperature (25°C) in a light:dark 12:12-h schedule. Four-week-old male C57BL/6 mice were fed a high-fat diet (Research Diets, 24% [w/w], 45% calories as fat) ad libitum for 7 weeks. Groups of mice were untreated, vehicle treated (calcium silicate), pair fed, or βL treated (p.o., micronized particles of βL coated with calcium silicate). Body weight and food intake were measured daily. At the end of experiments, one mouse from each group was anesthetized and examined by MRI. Other mice were dissected, and tissue weight was measured.

Antibodies, plasmids, and reagents. Anti-AMPKα antibody was purchased from Cell Signaling Technology (for immunoblotting) and Upstate (for immunoprecipitation). Anti–phospho-T172 AMPKα, anti–acetyl-CoA carboxylase (ACC), and anti–phospho-S79 ACC antibodies were from Cell Signaling Technology. Anti-NQO1 antibody was from Santa Cruz Biotechnology. Anti-OxPhos Complex II subunit antibody was from Molecular Probes. Anti–α-tubulin antibody was from Sigma. pEFIRES HA-NQO1, and pEFIRES HA-NQO1C609T plasmids were gifts from Dr. Gad Asher (Weizmann Institute of Science, Rehovot, Israel). Other reagents were purchased from Sigma, Calbiocam, or Amresco.

Liquid chromatography–mass spectroscopy/mass spectroscopy analysis. Cell extracts were prepared in 200 μl lysis buffer containing 80% ice-cold methanol/water ($MtOH/H_2O$). The cells were subjected to ultrasonication with a sonic Dismembator (Fisher Scientific, Fairland, NJ) on a power setting of 3 for 30 s. After centrifugation at 12,000 rpm for 10 min, the supernatant was filtered through a Microcon YM-3 filter (Millipore, Bedford, MA) at 4°C for 40 min and evaporated down to dryness using a Vacufuge Concentrator before reconstitution in 50 μl of water. The chromatographic system was set up as described in a previous work (15) with minor modifications. The mass spectrometer was operated in the negative ion mode with an electrospray voltage of 4,000 V at 300°C and was supplied by auxiliary gas (30 psi) (15). Quantification was performed with Xcalibur software (Thermo Fisher Scientific) using the standard addition method. Liver samples were extracted by perchloric acid ($HClO_4$) or potassium hydroxide (4) solution to determine adenine and oxidized and reduced pyridine nucleotide contents, respectively. Electrospray–ionization mass spectrometry was performed in positive ion mode using a MDS Sciex API 4000 Triple Quadrupole Mass Spectrometer (Applied Biosystems, Ontario, Canada) followed by chromatographic separation on an Agilent 1100 series high-performance liquid chromatography system (Agilent Technologies, Palo Alto, CA) equipped with an XTerra MS C_{18} 2.1 × 150 mm, 3.5-μm column (Waters, Milford, MA), as previously described (16).

Histochemistry and electron microscopy. Mouse tissues were fixed with formalin, dehydrated with ethanol, embedded in paraffin, and cut at a thickness of 5 μmol/l. Sections of epididymal fat, liver, soleus muscle, and extensor digitorum longus (EDL) were prepared for hematoxylin and eosin staining. Liver and muscle tissues were prepared as described previously (17) for transmission electron microscopy (Tecnai G2 Spirit Twin; FEI Company; Korea Basic Science Institute).

Enzyme assays. Cytoplasmic extracts were prepared from mouse tissues for enzyme assays. NQO1 activity was measured as described previously (14). This method measures the decrease in absorbance at 600 nm as a result of the

reduction of 2,6-dichlorophenolindophenol. Total AMPK activity was measured using a synthetic "SAMS" peptide substrate and [γ-^{32}P]ATP as described previously (18). ACC activity was estimated by quantifying the fixation of $^{14}CO_2$ to acid-stable products (19). Carnitine palmitoyltransferase (CPT) activity was measured by the transfer of ^{14}C-carnitine into the mitochondria matrix in L6 myoblasts and soleus muscle as described previously (19). Hydroxyacyl-CoA dehydrogenase (HAD) activity was measured in L6 myoblasts by monitoring the conversion of acetoacetyl-CoA to L-3-hydroxybutyryl CoA and the concomitant oxidation of NADH to NAD^+. The reaction was monitored at 340 nm as described previously (20).

Analysis of fatty acid oxidation and malonyl-CoA concentration. ^{14}C-palmityl-CoA (Perkin Elmer) oxidation by βL was measured in L6 myoblasts and soleus muscle using $^{14}CO_2$ and 0.2 ml of benzethonium solution as described previously (20). Malonyl-CoA was measured by high-performance liquid chromatography as described previously (21).

Analysis of physiological indicators. O_2 consumption was estimated as described previously (22). For indirect calorimetry, individual mice were placed in calorimetry chambers (Oxymax OPTO-M3 system; Columbus Instruments, Columbus, OH) and allowed to adapt for 48 h. During the first 24 h, mice had free access to food and water, and during the second 24 h, the mice had access to water only. Energy expenditure was calculated by measuring O_2 consumption and CO_2 production every 30 min for 24 h. For a cold-resistance test, DIO mice were exposed to 4°C ambient temperature for 12 h and rectal temperature was measured for 12 h. Blood samples were collected in heparinized tubes and separated by centrifugation and stored at −20°C for future use. Enzymatic colorimetry was used to quantify triglyceride, total cholesterol, free fatty acid, and glucose (Beckman Instruments, Palo Alto, CA). Plasma insulin (Linco Research, St. Charles, MO), TNFα (R&D System), adiponectin (Linco Research), resistin (KOMED), and leptin (Linco Research) were quantified by ELISA as described previously (4,23–25).

DNA microarray and quantitative RT-PCR. Microarray analysis was performed with pooled adipose, liver, or muscle tissue from adult male mice treated with vehicle or βL for 4 weeks. Total RNA was prepared from homogenized tissues using Trizol reagent (Invitrogen, Carlsbad, CA). Probes for microarray analysis were prepared from 10 μg of total RNA and hybridized to mouse 430A GeneChips (Affymetrix, Santa Clara, CA). The hybridized arrays were scanned and raw data extracted using Microarray Analysis Suite 5.0 (Affymetrix). For quantitative PCR, cDNA was reverse transcribed from 1 μg of total RNA with Superscript II and oligo primer (26). The resulting cDNAs were amplified using a LightCycler FastStart DNA Master SYBR Green I kit and LightCycler according to the manufacturer's instructions (Roche Diagnostics, Indianapolis, IN). Expression data were normalized to β-actin.

Immunoblotting. Total proteins from liver, muscle (EDL and soleus), and indicated cells were extracted in RIPA lysis buffer (500 mmol/l Tris-HCl pH 7.4, 1 mmol/l EDTA, 150 mmol/l NaCl, 1% NP-40, 0.25% Na-deoxycholate, and 1 mmol/l phenylmethylsulfonl fluoride), and content was determined using the Bio-Rad dye binding microassay (Bio-Rad Laboratories, Inc, Hercules, CA). Protein (20 μg per lane) was electrophoresed on a sodium dodecyl sulfate SDS-polyacrylamide gel after boiling for 5 min in SDS sample buffer. Proteins were blotted onto Hybond enhanced luminescence membranes (Amersham Pharmacia Biotech, Arlington Heights, IL). After electroblotting, the membranes were blocked with TBS and Tween 20 (10 mmol/l Tris-HCl pH 7.4, 150 mmol/l NaCl, and 0.1% Tween 20) containing 5% nonfat dry milk and incubated with the primary antibody diluted in blocking buffer overnight at 4°C. Membranes were then washed, incubated with the appropriate second antibodies for 1 h at room temperature, and rewashed. Blotted proteins were detected by using enhanced chemiluminescence.

Results are expressed as means ± SD. Differences between groups were examined for statistical significance using Student's t test and ANOVA. The difference was considered to be significant if $P < 0.05$.

RESULTS

Enhanced cytosolic NADH oxidation by NQO1 stimulates cellular energy metabolism. We screened natural compounds that induce NADH oxidation in the presence of NQO1. Interestingly, βL and its structurally related compounds, tanshinone 2A and cryptotanshinone, rapidly induced NADH oxidation in vitro (supplemental Fig. 1*A*, available in an online appendix at http://diabetes.diabetesjournals.org/cgi/content/full/db08-1183/DC1). In particular, βL strongly decreased the fluorescence intensity of NADH in NQO1-expressing HepG2 cells but not in NQO1-deficient HEK293 cells, suggesting that NQO1 is required for βL-induced NADH oxidation (supplemental Fig. 1*B*; available in the online appendix). Consistently, HEK293 cells transfected with wild-type NQO1 but not catalytically inactive NQO1 became responsive to βL (supplemental Fig. 1*B*, available in the online appendix). We measured total NAD^+ and NADH by the liquid chromatography–mass spectroscopy/mass spectroscopy method (15) in L6 muscle cells treated with different doses of βL. As expected, the NAD^+-to-NADH ratio was increased in L6 cells after βL treatment (Fig. 1*B*). These results indicate that βL induces NADH oxidation only in the presence of NQO1 activity.

Because the intracellular NAD^+-to-NADH ratio indicates the energy status of cells (27,28), βL-induced NADH oxidation may stimulate the AMPK signaling pathway, a well-known energy sensing pathway activated under energy depletion (6,7,29). In fact, βL treatment dramatically induced the activating phosphorylation in the catalytic subunit of AMPKα (AMPKα T172) within 30 min (Fig. 1*C* and supplemental Fig. 2*A*, available in the online appendix). Moreover, AMPK-dependent inhibitory phosphorylation of ACC (S79) was also strongly induced in βL-treated cells (Fig. 1*C* and supplemental Fig. 2*A*, available in the online appendix). To examine whether βL-induced AMPK activation requires NQO1 activity in vivo, we generated NQO1 knockout mice and injected βL into mouse embryonic fibroblasts (MEFs) isolated from the heterozygous (+/−) and homozygous (−/−) knockout mice. βL-induced phosphorylations of AMPK and ACC were not observed in NQO1-deficient MEFs but were observed in $NQO^{+/-}$ MEFs (Fig. 1*D–E*). Consistent with these immunoblot results, βL treatment modulated AMPK and ACC activities only in $NQO^{+/-}$ MEFs but not in $NQO^{-/-}$ MEFs (Fig. 1*D–E*). Furthermore, NQO1-specific inhibitors, dicoumarol and ES936, completely blocked βL-induced AMPK phosphorylation (supplemental Fig. 2*B*, available in the online appendix). These results collectively indicate that βL induces AMPK activation specifically by NQO1.

Because AMPK activation and concomitant ACC inhibition stimulate fatty acid oxidation (30,31), we measured the activities of two representative metabolic enzymes regulating mitochondrial fatty acid oxidation. Intriguingly, the activities of CPT and 3-HAD were significantly increased in βL-treated L6 myoblast cells (Fig. 1*F–G*). Consistently, mitochondrial fatty acid oxidation measured by ^{14}C-palmitoyl-CoA oxidation was substantially elevated in βL-treated cells (Fig. 1*H*). These results suggest that βL-induced NADH oxidation activates mitochondrial fuel metabolism by stimulating the AMPK signaling pathway.

Pharmacological NADH oxidation stimulates activation of AMP-activated protein kinase and fatty acid oxidation in vivo. To investigate the in vivo effects of βL, we examined βL-induced metabolic changes in DIO mice. Consistent with the cell data, βL treatment highly increased the NAD^+-to-NADH ratio in the liver of DIO mice (Fig. 2*A*). Moreover, βL treatment substantially increased the phosphorylations of AMPK and ACC and the activity of AMPK in the liver, EDL, and soleus muscle of DIO mice (Fig. 2*B–E*). We also monitored several enzymatic activities involved in mitochondrial fatty acid oxidation in the soleus muscle of βL-treated DIO mice. βL treatment significantly reduced the activity of ACC and the level of its metabolic product malonyl-CoA (32,33) in the soleus muscle (Fig. 2*F–G*). In contrast, the activities of CPT and HAD were highly increased in βL-treated mice compared with those of vehicle-treated mice (Fig. 2*H–I*). The rate of mitochondrial fatty acid oxidation was much higher in

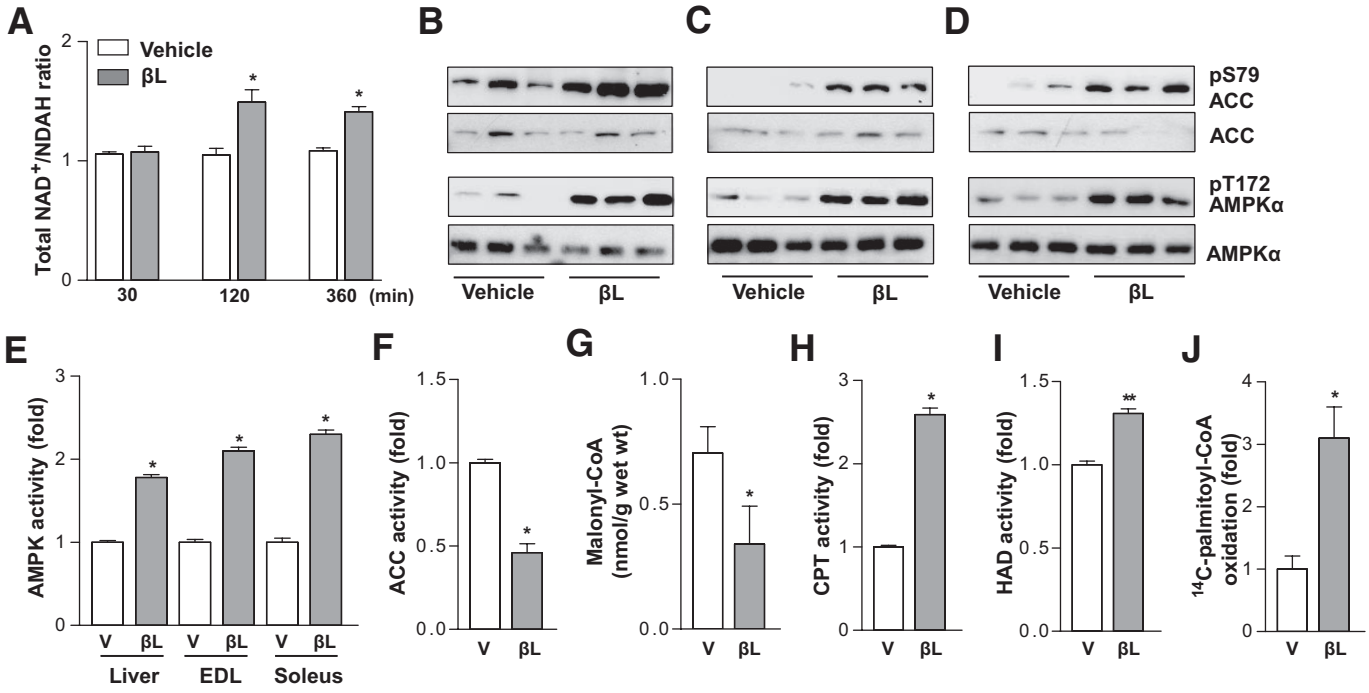

FIG. 2. βL activates AMP-activated protein kinase (AMPK) signaling pathway and fatty acid oxidation in vivo. *A*: NAD^+-to-NADH ratio was calculated in the liver of male mice treated intravenously with vehicle (n = 5; *open bars*) or 5 mg/kg βL (n = 5; *closed bars*) for the indicated time (*$P < 0.05$). *B–D*: Effects of βL on phosphorylations of AMPK and acetyl-CoA carboxylase (ACC) in vivo for liver (*B*), EDL (*C*), and soleus (*D*). DIO mice were dosed orally with vehicle (n = 3) or 50 mg/kg βL (n = 3). After treatment of βL for 2 h, extracts from liver (*B*), extensor digitorum longus (EDL) (*C*), and soleus muscle (*D*) were immunoblotted with antibodies against the indicated proteins. *E:* Comparison of the AMPK activity in the three indicated tissues of DIO mice dosed orally with vesicle and 50 mg/kg βL for 2 h (n = 5, respectively). *F–G*: Comparisons of the ACC activity (*F*) and malonyl-CoA quantity (*G*) in the soleus muscle of DIO mice dosed orally with vesicle and 50 mg/kg βL for 2 h (n = 5, respectively). *H–J*: βL stimulates mitochondrial energy metabolism in DIO mice. Comparisons of the carnitine palmitoyltransferase (CPT) (*H*), 3-HAD activities (*I*), or ^{14}C-palmityl-CoA oxidation (*J*) in vehicle and 50 mg/kg βL-treated DIO mice (n = 5, respectively). Mice used for all the experiments were male (*$P < 0.05$; **$P < 0.005$).

βL-treated mice (Fig. 2*J*). These data indicate that increased NADH oxidation by βL treatment stimulates the AMPK signaling pathway and mitochondrial fatty acid oxidation in vivo.

βL reverses obesity and related phenotypes in diet-induced obesity mice and *ob/ob* mice. To examine whether βL-induced NADH oxidation has a therapeutic potential in treating metabolic syndrome, we systematically treated DIO mice with βL for 8 weeks (Fig. 3, supplemental Fig. 3). Surprisingly, the body weight of βL-treated mice continuously decreased throughout the treatment, whereas that of the control mice slightly increased (Fig. 3*A*). Interestingly, the food intake of βL-treated mice decreased during the first 2 weeks of treatment and then returned to the normal state (Fig. 3*B*) because βL-treated mice exhibited progressive weight loss even after returning to the normal state of food intake (Fig. 3*A–B*). To observe the role of decreased food intake in the early phase of βL administration, we compared the body weight of the βL-treated group with that of the pair-fed group. In Fig. 3*C*, the treated group (n = 8) and pair-fed group (n = 8) showed 24.9 ± 7.36% and −3.4 ± 7.86% weight loss compared with the baseline weight. A comparison of the weights of the treated and pair-fed groups to those of the vehicle group showed that the βL-treated and pair-fed groups had weight losses of 33.6 ± 5.78% and 10.5 ± 3.00%, respectively; thus, ~23% of total weight loss can be attributed to the peripheral actions of βL (Fig. 3*C*, supplemental Fig. 3). These findings suggest that a major factor governing body weight loss in βL-treated mice is likely to be increased energy expenditure rather than decreased food intake.

Consistent with the decreased body weight, MRI of the coronal and transverse sections of βL-treated DIO mice showed dramatic decreases in subcutaneous and visceral adipose tissues (Fig. 3*D*). Moreover, the weights of subcutaneous, mesenteric, perirenal, and gonadal fats in βL-treated DIO mice were considerably decreased (supplemental Fig. 4), indicating that their body weight loss is the result of the reduced adipose tissues. After analyzing various indicators of glucose and fat metabolism in the sera of βL-treated DIO mice, we found overall decreased amounts of triglyceride, cholesterol, free fatty acid, glucose, insulin, adiponectin, resistin, and leptin in βL-treated DIO mice (Table 1). Notably, the adipocyte marker perilipin staining revealed that the size of lipid droplets in the epididymal fat cells was much smaller in βL-treated DIO mice (Fig. 3*E*). Moreover, oil red O staining in the liver showed that βL treatment considerably suppressed the liver steatosis in DIO mice (Fig. 3*F*). All these dramatic metabolic changes, including reduced body weight and adipocyte size, and decreased hepatic steatosis were similarly observed in βL-treated *ob/ob* mice (Fig. 4*A–D*). Consistently, βL treatment resulted in enhanced glucose disposal rates and improved insulin sensitivity in both DIO mice and Otsuka Long Evans Tokushima fatty type 2 diabetic model rats (supplemental Fig. 5).We conclude that βL treatment can alleviate the key symptoms of metabolic syndrome in the rodent models with obesity and diabetes.

Pharmacological NADH oxidation modulates expression of genes involved in metabolism and mitochondrial functions. To further understand the underlying mechanisms of βL-induced metabolic improvements, we performed genomewide microarray analyses in the liver,

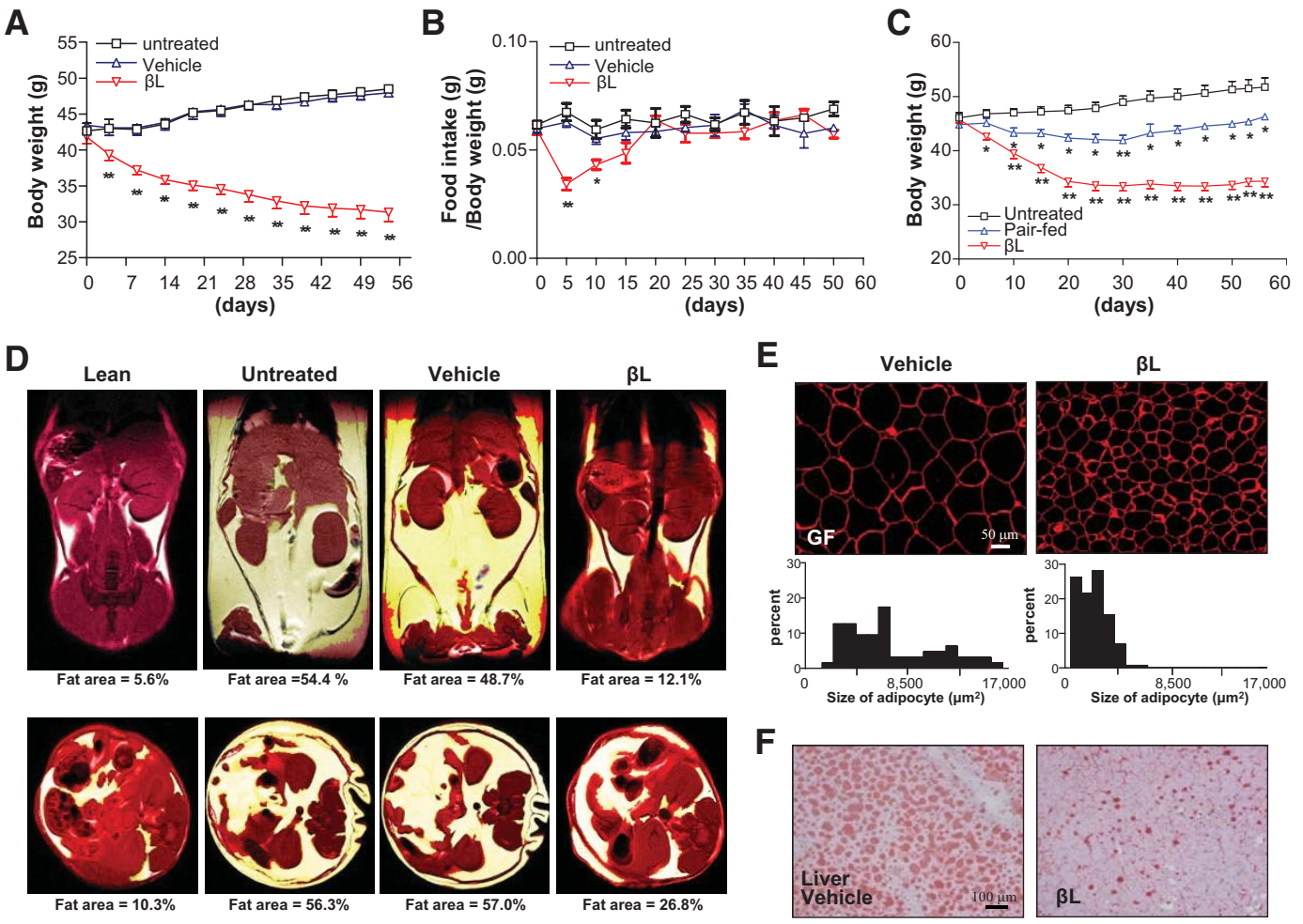

FIG. 3. βL treatment ameliorates the metabolic symptoms of DIO mice. *A–B*: The body weights (*A*) and the ratios of food intake to body weight (*B*) of the untreated (□; $n = 30$), vehicle-treated (△; $n = 42$), and βL-treated (▽; $n = 48$) groups were monitored during the oral administration of 50 mg · kg^{-1} · day^{-1} βL for 8 weeks. *C*: The body weight of the untreated (□; $n = 6$), pair-fed (△; $n = 8$), and 50 mg · kg^{-1} · day^{-1} βL-treated (▽; $n = 8$) groups, were monitored for 8 weeks after oral administration of βL (*$P < 0.05$; **$P < 0.005$). *D*: Representative MRI of the coronal (*upper panel*) and transverse (*lower panel*) sections in the four indicated mice groups. DIO mice were orally administered vehicle or 50 mg · kg^{-1} · day^{-1} βL for 8 weeks. Lean mice were used as control for a normal fat concentration. *E*: The sizes of lipid droplets in gonadal fat (GF) were compared between DIO mice treated with vehicle (*left*) and 50 mg · kg^{-1} · day^{-1} βL (*right*) for 4 weeks. Immunostaining with anti-perilipin antibody (red) was used to measure the size of lipid droplets. *F*: Oil red O staining (*red*) in the liver from DIO mice treated with vehicle (*upper*) or 50 mg · kg^{-1} · day^{-1} βL (*lower*) for 4 weeks was used to evaluate hepatic steatosis. Mice used for all the experiments were male (*$P < 0.05$; **$P < 0.005$). (A high-quality digital representation of this figure is available in the online issue.)

muscle, and adipose tissues of βL-treated DIO mice. Genes involved in metabolism and mitochondrial functions were differentially expressed in DIO mice exposed to βL, and quantitative RT-PCR experiments also verified these results (Table 2). For example, βL treatment strongly induced PGC-1α and nuclear respiratory factor-1, the master regulators of mitochondrial biogenesis (34,35), in the liver and muscle of DIO mice. In addition, mitochondrial metabolic genes (COX4 and COX7) were also upregulated in the muscle of βL-treated DIO mice. Interestingly, Sirt1 and Sirt3, which are known to be activated in response to calorie restriction (5,36,37), were also highly induced in the muscle of βL-treated mice. Moreover, genes related to lipolysis (LPL and ATGL) and glucose uptake (GLUT4) were upregulated in the adipose tissue of βL-treated DIO mice. However, fatty acid synthase and PPARγ, which play key roles in adipogenesis and fatty acid synthesis (38), were downregulated in βL-treated DIO mice. These results strongly suggest that βL-induced NADH oxidation stimulates mitochondrial biogenesis and functions and also enhances energy metabolism by controlling global gene expression related to cellular metabolism.

TABLE 1
Metabolic parameters in mice treated with vehicle or βL

	Vehicle	βL
Triglyceride (mg/dl)	80.8 ± 10.57	66.33 ± 7.66*
Cholesterol (mg/dl)	219.8 ± 52.84	140 ± 19.34**
Free fatty acid (uEq/l)	1085 ± 174.1	487 ± 69.26**
Adiponectin (ng/ml)	21.74 ± 4.63	8.4 ± 1.02**
Resistin (ng/ml)	1.458 ± 0.23	1 ± 0.27**
TNFa (pg/ml)	19.88 ± 4.03	22.82 ± 7.1
Leptin (ng/ml)	128.8 ± 13.85	33.47 ± 17.56**
Glucose (mg/dl)	232.8 ± 15.78	133.3 ± 33.66**
Insulin (ng/dl)	4.1 ± 1.49	1.68 ± 0.95**

Data are means ± SD. After oral administration with vehicle ($n = 5$) or βL ($n = 6$) for 4 weeks, metabolic parameters were analyzed. *$P < 0.05$, **$P < 0.005$ for the βL-treated group versus the vehicle control group.

Long-term pharmacological NADH oxidation stimulates mitochondrial biogenesis and energy expenditure. Because several genes affected by βL treatment take part in

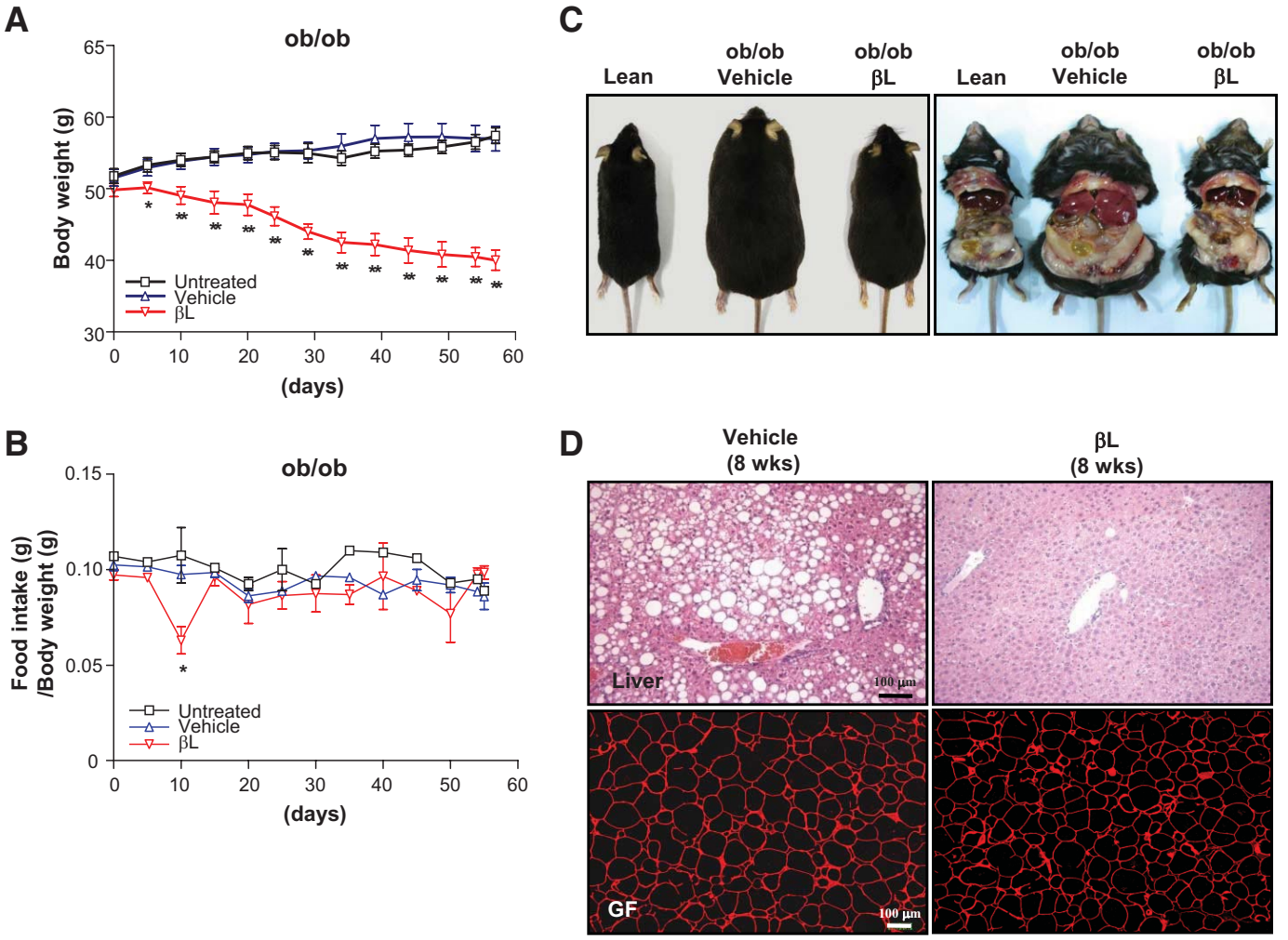

FIG. 4. The effects of βL on various metabolic symptoms in *ob/ob* mice. *A* and *B*: The body weight (*A*) and the ratio of food intake to body weight (*B*) of the untreated (□; $n = 4$), vehicle-treated (△; $n = 8$), and 200 mg · kg^{-1} · day^{-1} βL-treated (▽; $n = 8$) groups, were monitored for 8 weeks after oral administration of βL (*$P < 0.05$; **$P < 0.005$). *C*: The photographic images of lean, vehicle-treated, and 200 mg · kg^{-1} · day^{-1} βL-treated *ob/ob* mice after 8 weeks of treatment. *D*: Tissue sections of the liver (*upper panel*) and gonadal fat (GF, *lower panel*) of *ob/ob* mice treated with vehicle (*left panel*) or 200 mg · kg^{-1} · day^{-1} βL (*right panel*) for 8 weeks were stained with hematoxylin and eosin (*upper panel*) and anti-perilipin antibody (*lower panel*), respectively. (A high-quality digital representation of this figure is available in the online issue.)

mitochondrial remodeling and biogenesis (34,39,40), we examined the physiological and ultrastructural changes of mitochondria in βL-treated DIO mice. As a result, mitochondria in the liver of untreated DIO mice appeared to be swollen, distorted, and deficient in cristae and matrix (Fig. 5*A–B*). However, DIO mice treated with βL for 8 weeks showed an increased number of mitochondria with normal morphologies such as well-organized cristae and matrix structures (Fig. 5*A–B*). Furthermore, the mitochondria collected from the soleus muscle in βL-treated DIO mice exhibited higher levels of mitochondrial DNA and complex II subunit expression compared with those in untreated controls, suggesting that βL treatment actively induced mitochondrial biogenesis (Fig. 5*C*). Consistently, the number of fibers in the soleus muscle that showed strong ATPase staining intensity and intermyofibrillar mitochondria was increased in βL-treated DIO mice (Fig. 5*D*).

To further characterize the physiological effects of mitochondrial restoration in βL-treated DIO mice, we measured two metabolic indices: respiratory oxygen consumption and cold resistance. The quantity of resting oxygen uptake (Vo_2) was markedly increased after adjusting for body weight in βL-treated DIO mice (Fig. 5*E*), whereas the ratio of night respiratory exchange was decreased (0.77, βL-treated mice; 0.82, control mice; $P < 0.005$, data not shown). However, Vo_2 that had not been adjusted for body weight showed no statistical significance between control and βL-treated groups. Thus, adipose tissue mass, which is profoundly decreased by βL treatment, may be an important denominator for the analysis of resting Vo_2. In addition, βL-treated DIO mice displayed much stronger cold resistance than the control mice (Fig. 5*F*). More importantly, βL treatment significantly increased energy expenditure of DIO mice (Fig. 5*G*). Overall, these results propose that increases in mitochondrial integrity, oxygen consumption, and energy expenditure are the underlying mechanisms of βL in assuaging the metabolic symptoms of DIO mice.

DISCUSSION

NAD^+ and its derivatives are classic metabolites involved in energy metabolism (11). Recent evidence suggests that NAD^+ is a central regulator in cellular energy metabolism. Moreover, the importance of cellular NAD^+ levels has been highlighted by the discovery of SIR2-related proteins

TABLE 2
Expression of genes related to energy metabolism and mitochondrial functions in the liver, muscle, and white adipose tissue

Tissue	Genes	Relative mRNA levels (βL/vehicle group)
Liver	*PGC1α*	3.46 ± 2.1*
	NRF-1	1.88 ± 0.38*
	mtTFA	1.32 ± 0.32
	CPT1	1.56 ± 0.29*
	UCP2	3.06 ± 0.67**
	AMPKα1	1.84 ± 0.64*
	AMPKα2	1.42 ± 0.39
	PPARγ	1.00 ± 0.25
Muscle	*PGC1α*	1.70 ± 0.31*
	NRF-1	1.60 ± 0.42*
	mtTFA	0.81 ± 0.45
	CPT1	1.07 ± 0.48
	COX4	2.18 ± 0.45*
	COX7	1.69 ± 0.36
	GLUT2	5.08 ± 4.55
	GLUT4	1.45 ± 0.89
	PPARα	1.45 ± 0.42
	AMPKα1	2.80 ± 1.71
	AMPKα2	1.69 ± 1.33
	SIRT1	2.05 ± 0.44*
	SIRT3	3.33 ± 0.84*
	UCP2	2.27 ± 1.22
	UCP3	2.78 ± 1.75
Gonadal fat (WAT)	*PGC1α*	2.02 ± 0.3**
	NRF-1	1.71 ± 1.08
	FASN	0.32 ± 0.13*
	LPL	2.12 ± 0.37**
	ATGL	2.34 ± 0.38**
	SCD1	0.68 ± 0.26
	AOX	1.58 ± 0.4*
	GLUT2	2.10 ± 1.2
	GLUT4	5.20 ± 0.82**
	PPARα	2.36 ± 0.32**
	PPARγ	0.51 ± 0.23*
	SIRT1	1.45 ± 0.18**
	SIRT2	1.33 ± 0.15**
	SIRT3	4.33 ± 0.91*

Data are means ± SD. After oral administration with vehicle ($n = 5$) or βL ($n = 6$) for 4 weeks, relative mRNA levels in the indicated tissues were analyzed by quantitative RT-PCR. The values indicate relative mRNA levels of βL-treated groups compared to those of vehicle control groups. *$P < 0.05$, **$P < 0.005$ for the βL-treated group versus the vehicle control group.

(sirtuins) that mediate calorie-restriction responses in yeast and mammals (41). Yeast Sir2 and a mammalian ortholog sirtuin, Sirt1, are NAD^+-dependent deacetylases that are regulated by the NAD^+-to-NADH ratio (5). Accumulating evidence has suggested that NAD^+-to-NADH ratios are altered in various pathological conditions such as neurodegeneration, diabetes, and oxidative stress (28,42). The pharmacological activation of NAD^+-dependent SirT1 compensates for the effects of a high-calorie diet (10). Based on these observations, pharmacological induction of higher NAD^+-to-NADH would be expected to ameliorate the metabolic syndrome.

NQO1 is a flavoenzyme that uses NAD(P)H as an electron donor to catalyze the reduction of substrates. Previous studies and our data suggest that βL is a specific and high-affinity substrate of NQO1 in vitro and in vivo (14). βL would therefore have the propensity to induce a higher NAD^+-to-NADH ratio. The expression of NQO1, a target of βL, is highly upregulated in liver, muscle, and fat tissues, which are important for the regulation of whole-body energy metabolism and insulin sensitivity (supplemental Fig. 6). The promoter of the NQO1 gene has an antioxidant response element that serves as the binding motif for the factor Nrf2, which is activated by reactive oxygen species (ROS) stimuli. The increased ROS stimulation in metabolically active tissues under obesity and diabetic conditions may activate Nrf2 and NQO1 gene expression. Consistently, Palming et al. (43) found that human adipocytes have high NQO1 expression and that NQO1 expression levels were positively correlated with adiposity, glucose tolerance, and markers of liver dysfunction. Taken together, NQO1 would appear to be a useful pharmacological target for the induction of higher NAD^+-to-NADH ratios in obesity and diabetes models.

We have shown that the enhanced NADH oxidation induced by βL in NQO1-present cells increases phosphorylation and activation of AMPK. The reduced cytosolic NADH levels induced by βL treatment may disturb the proper distribution of NADH reducing equivalents in mitochondrial complexes for energy production, suggesting that βL may transiently increase AMP levels and activate AMPK to compensate for cellular energy depletion (10,36,44). Two upstream kinases, LKB1 and CaMKK, are involved in the phosphorylation of the catalytic subunit of AMPK (45,46). We tested the effects of βL on AMPK phosphorylation in LKB1-deficient MEFs. AMPK phosphorylation was only observed at very early time points (30 s to 5 min) after treatment with βL in LKB1-deficient cells (data not shown). This pattern of AMPK activation is quite different from that observed in cells with normal LKB1 expression (supplemental Fig. 2*A*), in which βL resulted in prolonged AMPK phosphorylation. The CaMKK inhibitor (STO609) completely abolished the early phase of AMPK phosphorylation (data not shown). These findings strongly suggest that both LKB1 and CaMKK are required for full activation of AMPK under βL-induced AMPK phosphorylation conditions. Activation of AMPK led to increased fatty acid oxidation by inactivating ACC phosphorylation. Consistently, βL-mediated AMPK activation induces ACC phosphorylation and activation of CPT and HAD, resulting in beneficial fatty acid oxidation. Taken together, these findings suggest that pharmacological stimulation of NADH oxidation leads to increased mitochondrial fatty acid oxidation.

We additionally examined whether βL-induced NADH oxidation could be used as a therapy for treating obesity, a major component of metabolic syndrome. Pair-feeding studies (Fig. 3*C*, supplemental Fig. 3) clearly demonstrated that loss of weight induced by βL is mediated by both central and peripheral actions. Although a decrease of food intake after βL treatment was noted in the early phase of treatment, food intake recovered with continued βL administration. We found that intracranial administration of βL in mice resulted in a dramatic decrease in feeding behavior (data not shown); however, it is unclear which mechanism in the hypothalamus mediates the βL-induced decrease in food intake. Long-term weight loss induced by βL is mainly the result of the peripheral action of βL and its weight-reducing effect, which are accompanied by a smaller fat mass; lower fatty infiltration in the liver; decreased levels of plasma insulin, triglyceride, and glucose; and increased glucose disposal rates after insulin

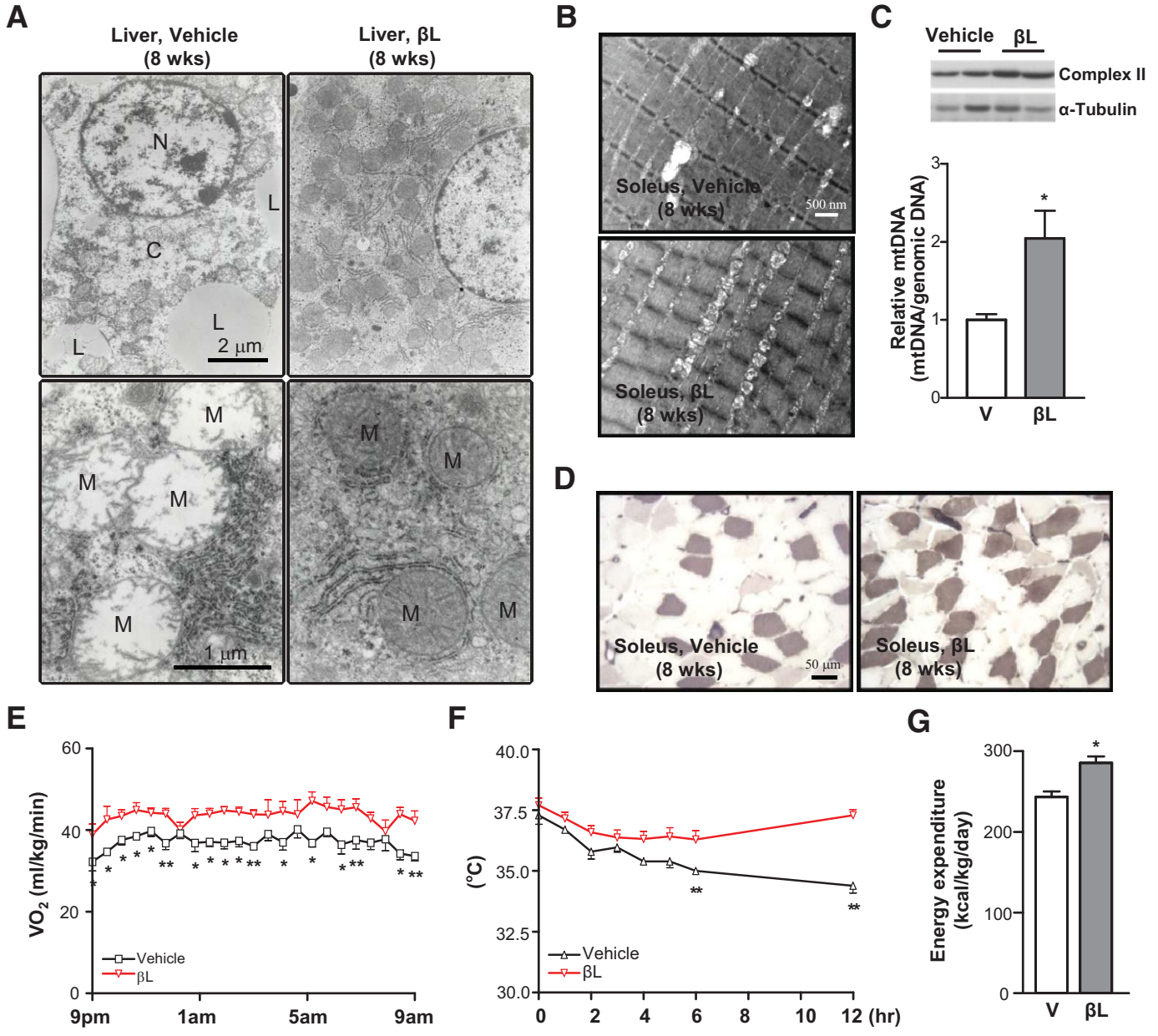

FIG. 5. Long-term βL treatment stimulates mitochondrial remodelling and biogenesis and increases energy expenditure. *A* and *B*: Transmission electron microscopic images of the liver (*A*) and soleus muscle (*B*) of DIO mice treated with vehicle or 50 mg · kg^{-1} · day^{-1} βL for 8 weeks. N, nucleus; L, lipid droplets; C, cytosol; M, mitochondria. *C*: Immunoblot analysis against complex II subunit (*upper panel*) and quantitative RT-PCR analysis for mitochondrial DNA (mtDNA) contents (*lower panel*) were performed in the soleus muscle of DIO mice treated with vehicle ($n = 5$) or 50 mg · kg^{-1} · day^{-1} βL ($n = 5$). α-Tubulin was used as loading control. *D*: pH-sensitive ATPase staining (*pale purple*) of histological sections was performed in the soleus muscle of DIO mice treated with vehicle (*left*) and βL (*right*). *E* and *F*: Oxygen consumption (Vo_2) (*E*) and cold resistance (*F*) were compared between DIO mice treated with vehicle (□; $n = 5$) or 50 mg · kg^{-1} · day^{-1} βL (▽; $n = 5$) for 8 weeks. *G*: Comparison of the energy expenditure between DIO mice treated with vehicle and βL. Mice used for all the experiments were male (*$P < 0.05$; **$P < 0.005$). (A high-quality digital representation of this figure is available in the online issue.)

treatment. These results suggest that the increased NADH oxidation induced by βL could lead to an amelioration of key components of metabolic syndrome in rodent models with obesity and diabetes.

The reversal of obesity and other phenotypes of DIO and *ob/ob* mice by βL is associated with the normalization of disorganized mitochondrial ultrastructure and increased numbers of mitochondria. Mitochondrial dysfunctions are frequently associated with obesity and diabetes, and improvements in obesity and glucose tolerance are associated with enhanced mitochondrial oxphos functions and biogenesis (47,48). En examination of the gene expression patterns after βL treatment showed increased expression of PGC-1α and SirT family genes in liver, muscle, and adipose tissues. Prolonged AMPK activation is known to increase PGC-1α expression, SirT1 activity, and mitochondrial biogenesis. Taken together, it is plausible that AMPK activation by βL induces PGC-1α, a master regulator of mitochondrial biogenesis, and Sirt1, a mediator of calorie-restriction effects, which promote higher mitochondrial biogenesis and energy expenditure in mice. The resting Vo_2 was found to be higher in the βL-treated group than in the vehicle group after adjusting for body weight. However, this finding does not necessarily indicate that βL treatment increases resting metabolic rate because changes of body weight, including fat mass, may affect

resting V_{O_2}. To find the effects of βL treatment on metabolic rate, additional analysis of submaximal and maximal V_{O_2} with or without adjustments for body composition will be required. The consequences of long-term physiological adaptations on enhanced NADH oxidation after βL treatment will require further study to prove the potential of βL as a new treatment for obesity and diabetes.

Previous studies showed that βL inhibits tumorigenesis and that NQO1 mediates this effect of βL (13,14). Interestingly, the cytotoxic effect of βL was prominently observed in cultured cancer cells, whereas it was barely detectable in normal primary cultured cells (supplemental Fig. 7) (49). Although primary cultured MEFs showed strong resistance to βL cytotoxicity, ~10% of the MEFs underwent cell death (supplemental Figs. 7 and 8). This phenomenon was completely suppressed by adding palmitate to the culture medium (supplemental Fig. 8), suggesting that increased palmitate oxidation compensates βL cytotoxicity. These data suggest that βL-induced cell death occurs selectively in cancer cells that exhibit reduced mitochondrial oxidative phosphorylation. Although the systemic toxicity of βL in humans has not been fully established, ARQ501, a synthetic version of βL, has been subjected to phase I and II clinical trials and only mild adverse effects such as anemia and fatigue have been observed. It is indispensable to evaluate the systemic toxicity of βL using different administration routes, formulas, and exposure times.

ACKNOWLEDGMENTS

This research was supported by the Korea Science and Engineering Foundation (KOSEF) (M10753020001-07N5302-0110), the Ministry of Education, Science and Technology, MarineBio Research Grant B10400207A290100210, and a Ministry of Maritime and Fisheries and KT&G grant, Korea. J.H.H. and Y.K.K. were supported by the second phase of the BK21 program, Ministry of Education, Korea. I.K.L. was supported by the National Research Laboratory program (grant M106 00000271-06J000-27110) from KOSEF, Ministry of Education, Science and Technology, Korea. J.C. was supported by a National Creative Research Initiatives grant (M01080206) from KOSEF, Ministry of Education, Science and Technology, Korea.

No potential conflicts of interest relevant to this article were reported.

We thank Young Mi Kang, Ki Nam Min, and Jong Kuk Park for technical assistance and animal care.

REFERENCES

1. Kahn R, Buse J, Ferrannini E, Stern M: The metabolic syndrome: time for a critical appraisal: joint statement from the American Diabetes Association and the European Association for the Study of Diabetes. *Diabetes Care* 28:2289–2304, 2005
2. Despres JP, Lemieux I: Abdominal obesity and metabolic syndrome. *Nature* 444:881–887, 2006
3. Knowler WC, Barrett-Connor E, Fowler SE, Hamman RF, Lachin JM, Walker EA, Nathan DM: Reduction in the incidence of type 2 diabetes with lifestyle intervention or metformin. *N Engl J Med* 346:393–403, 2002
4. Shklyaev S, Aslanidi G, Tennant M, Prima V, Kohlbrenner E, Kroutov V, Campbell-Thompson M, Crawford J, Shek EW, Scarpace PJ, Zolotukhin S: Sustained peripheral expression of transgene adiponectin offsets the development of diet-induced obesity in rats. *Proc Natl Acad Sci U S A* 100:14217–14222, 2003
5. Guarente L, Picard F: Calorie restriction—the SIR2 connection. *Cell* 120:473–482, 2005
6. Hardie DG: AMP-activated protein kinase as a drug target. *Annu Rev Pharmacol Toxicol* 47:185–210, 2007
7. Kahn BB, Alquier T, Carling D, Hardie DG: AMP-activated protein kinase: ancient energy gauge provides clues to modern understanding of metabolism. *Cell Metab* 1:15–25, 2005
8. Lin J, Handschin C, Spiegelman BM: Metabolic control through the PGC-1 family of transcription coactivators. *Cell Metab* 1:361–370, 2005
9. Guarente L: Sirtuins as potential targets for metabolic syndrome. *Nature* 444:868–874, 2006
10. Baur JA, Pearson KJ, Price NL, Jamieson HA, Lerin C, Kalra A, Prabhu VV, Allard JS, Lopez-Lluch G, Lewis K, Pistell PJ, Poosala S, Becker KG, Boss O, Gwinn D, Wang M, Ramaswamy S, Fishbein KW, Spencer RG, Lakatta EG, Le Couteur D, Shaw RJ, Navas P, Puigserver P, Ingram DK, de Cabo R, Sinclair DA: Resveratrol improves health and survival of mice on a high-calorie diet. *Nature* 444:337–342, 2006
11. Berger F, Ramirez-Hernandez MH, Ziegler M: The new life of a centenarian: signalling functions of NAD(P). *Trends Biochem Sci* 29:111–118, 2004
12. Pollak N, Dolle C, Ziegler M: The power to reduce: pyridine nucleotides—small molecules with a multitude of functions. *Biochem J* 402:205–218, 2007
13. Jaiswal AK: Regulation of genes encoding NAD(P)H:quinone oxidoreductases. *Free Radic Biol Med* 29:254–262, 2000
14. Pink JJ, Planchon SM, Tagliarino C, Varnes ME, Siegel D, Boothman DA: NAD(P)H:Quinone oxidoreductase activity is the principal determinant of beta-lapachone cytotoxicity. *J Biol Chem* 275:5416–5424, 2000
15. Ni Q, Reid KR, Burant CF, Kennedy RT: Capillary LC-MS for high sensitivity metabolomic analysis of single islets of Langerhans. *Anal Chem* 80:3539–3546, 2008
16. Lazzarino G, Amorini AM, Fazzina G, Vagnozzi R, Signoretti S, Donzelli S, Di Stasio E, Giardina B, Tavazzi B: Single-sample preparation for simultaneous cellular redox and energy state determination. *Anal Biochem* 322:51–59, 2003
17. Picard F, Gehin M, Annicotte J, Rocchi S, Champy MF, O'Malley BW, Chambon P, Auwerx J: SRC-1 and TIF2 control energy balance between white and brown adipose tissues. *Cell* 111:931–941, 2002
18. Hayashi T, Hirshman MF, Fujii N, Habinowski SA, Witters LA, Goodyear LJ: Metabolic stress and altered glucose transport: activation of AMP-activated protein kinase as a unifying coupling mechanism. *Diabetes* 49:527–531, 2000
19. Dobrzyn P, Dobrzyn A, Miyazaki M, Cohen P, Asilmaz E, Hardie DG, Friedman JM, Ntambi JM: Stearoyl-CoA desaturase 1 deficiency increases fatty acid oxidation by activating AMP-activated protein kinase in liver. *Proc Natl Acad Sci U S A* 101:6409–6414, 2004
20. Oh W, Abu-Elheiga L, Kordari P, Gu Z, Shaikenov T, Chirala SS, Wakil SJ: Glucose and fat metabolism in adipose tissue of acetyl-CoA carboxylase 2 knockout mice. *Proc Natl Acad Sci U S A* 102:1384–1389, 2005
21. Hosokawa Y, Shimomura Y, Harris RA, Ozawa T: Determination of short-chain acyl-coenzyme A esters by high-performance liquid chromatography. *Anal Biochem* 153:45–49, 1986
22. Zhang X, Xie YW, Nasjletti A, Xu X, Wolin MS, Hintze TH: ACE inhibitors promote nitric oxide accumulation to modulate myocardial oxygen consumption. *Circulation* 95:176–182, 1997
23. Pajvani UB, Trujillo ME, Combs TP, Iyengar P, Jelicks L, Roth KA, Kitsis RN, Scherer PE: Fat apoptosis through targeted activation of caspase 8: a new mouse model of inducible and reversible lipoatrophy. *Nat Med* 11:797–803, 2005
24. Nonogaki K, Strack AM, Dallman MF, Tecott LH: Leptin-independent hyperphagia and type 2 diabetes in mice with a mutated serotonin 5-HT2C receptor gene. *Nat Med* 4:1152–1156, 1998
25. Asselin-Paturel C, Boonstra A, Dalod M, Durand I, Yessaad N, Dezutter-Dambuyant C, Vicari A, O'Garra A, Biron C, Briere F, Trinchieri G: Mouse type I IFN-producing cells are immature APCs with plasmacytoid morphology. *Nat Immunol* 2:1144–1150, 2001
26. Schaffner-Sabba K, Schmidt-Ruppin KH, Wehrli W, Schuerch AR, Wasley JW: beta-Lapachone: synthesis of derivatives and activities in tumor models. *J Med Chem* 27:990–994, 1984
27. Ying W: NAD+ and NADH in cellular functions and cell death. *Front Biosci* 11:3129–3148, 2006
28. Ido Y: Pyridine nucleotide redox abnormalities in diabetes. *Antioxid Redox Signal* 9:931–942, 2007
29. Lee JH, Koh H, Kim M, Kim Y, Lee SY, Karess RE, Lee SH, Shong M, Kim JM, Kim J, Chung J: Energy-dependent regulation of cell structure by AMP-activated protein kinase. *Nature* 447:1017–1020, 2007
30. Carling D, Zammit VA, Hardie DG: A common bicyclic protein kinase cascade inactivates the regulatory enzymes of fatty acid and cholesterol biosynthesis. *FEBS Lett* 223:217–222, 1987
31. Hardie DG, Pan DA: Regulation of fatty acid synthesis and oxidation by the AMP-activated protein kinase. *Biochem Soc Trans* 30:1064–1070, 2002
32. Ruderman N, Flier JS: Cell biology. Chewing the fat—ACC and energy balance. *Science* 291:2558–2559, 2001

33. Abu-Elheiga L, Matzuk MM, Abo-Hashema KA, Wakil SJ: Continuous fatty acid oxidation and reduced fat storage in mice lacking acetyl-CoA carboxylase 2. *Science* 291:2613–2616, 2001
34. Wu Z, Puigserver P, Andersson U, Zhang C, Adelmant G, Mootha V, Troy A, Cinti S, Lowell B, Scarpulla RC, Spiegelman BM: Mechanisms controlling mitochondrial biogenesis and respiration through the thermogenic coactivator PGC-1. *Cell* 98:115–124, 1999
35. Evans MJ, Scarpulla RC: NRF-1: a trans-activator of nuclear-encoded respiratory genes in animal cells. *Genes Dev* 4:1023–1034, 1990
36. Cohen HY, Miller C, Bitterman KJ, Wall NR, Hekking B, Kessler B, Howitz KT, Gorospe M, de Cabo R, Sinclair DA: Calorie restriction promotes mammalian cell survival by inducing the SIRT1 deacetylase. *Science* 305:390–392, 2004
37. Shi T, Wang F, Stieren E, Tong Q: SIRT3, a mitochondrial sirtuin deacetylase, regulates mitochondrial function and thermogenesis in brown adipocytes. *J Biol Chem* 280:13560–13567, 2005
38. Kim JB, Spiegelman BM: ADD1/SREBP1 promotes adipocyte differentiation and gene expression linked to fatty acid metabolism. *Genes Dev* 10:1096–1107, 1996
39. Lowell BB, Spiegelman BM: Towards a molecular understanding of adaptive thermogenesis. *Nature* 404:652–660, 2000
40. Reznick RM, Shulman GI: The role of AMP-activated protein kinase in mitochondrial biogenesis. *J Physiol* 574:33–39, 2006
41. Lin SJ, Ford E, Haigis M, Liszt G, Guarente L: Calorie restriction extends yeast life span by lowering the level of NADH. *Genes Dev* 18:12–16, 2004
42. Ying W: NAD+-to-NADH and NADP+-to-NADPH in cellular functions and cell death: regulation and biological consequences. *Antioxid Redox Signal* 10:179–206, 2008
43. Palming J, Sjoholm K, Jernas M, Lystig TC, Gummesson A, Romeo S, Lonn L, Lonn M, Carlsson B, Carlsson LM: The expression of NAD(P)H: quinone oxidoreductase 1 is high in human adipose tissue, reduced by weight loss, and correlates with adiposity, insulin sensitivity, and markers of liver dysfunction. *J Clin Endocrinol Metab* 92:2346–2352, 2007
44. Hardie DG, Carling D: The AMP-activated protein kinase—fuel gauge of the mammalian cell? *Eur J Biochem* 246:259–273, 1997
45. Woods A, Dickerson K, Heath R, Hong SP, Momcilovic M, Johnstone SR, Carlson M, Carling D: Ca2+/calmodulin-dependent protein kinase kinase-beta acts upstream of AMP-activated protein kinase in mammalian cells. *Cell Metab* 2:21–33, 2005
46. Hawley SA, Pan DA, Mustard KJ, Ross L, Bain J, Edelman AM, Frenguelli BG, Hardie DG: Calmodulin-dependent protein kinase kinase-beta is an alternative upstream kinase for AMP-activated protein kinase. *Cell Metab* 2:9–19, 2005
47. Pospisilik JA, Knauf C, Joza N, Benit P, Orthofer M, Cani PD, Ebersberger I, Nakashima T, Sarao R, Neely G, Esterbauer H, Kozlov A, Kahn CR, Kroemer G, Rustin P, Burcelin R, Penninger JM: Targeted deletion of AIF decreases mitochondrial oxidative phosphorylation and protects from obesity and diabetes. *Cell* 131:476–491, 2007
48. Lagouge M, Argmann C, Gerhart-Hines Z, Meziane H, Lerin C, Daussin F, Messadeq N, Milne J, Lambert P, Elliott P, Geny B, Laakso M, Puigserver P, Auwerx J: Resveratrol improves mitochondrial function and protects against metabolic disease by activating SIRT1 and PGC-1alpha. *Cell* 127:1109–1122, 2006
49. Li Y, Sun X, LaMont JT, Pardee AB, Li CJ: Selective killing of cancer cells by beta-lapachone: direct checkpoint activation as a strategy against cancer. *Proc Natl Acad Sci U S A* 100:2674–2678, 2003